

# Optimal One-bit Quantizers are Asymmetric for Additive Uniform Noise

Gholamreza Alirezaei and Rudolf Mathar  
 Institute for Theoretical Information Technology  
 RWTH Aachen University, D-52056 Aachen, Germany  
 {alirezaei, mathar}@ti.rwth-aachen.de

**Abstract**—In this paper, we consider one-bit output quantization of an amplitude bounded input-signal subject to arbitrary additive noise. Capacity is then represented in various ways, each demonstrating that finding the optimum quantization threshold  $q$  is an extremely difficult problem. For a class of noise distributions, of which a typical representative is the uniform distribution, it is shown that the optimum quantizer is asymmetric. This contradicts intuition, which for symmetric noise expects the optimum threshold to be the average of the input distribution.

## I. INTRODUCTION AND MOTIVATION

A/D converters often encounter noise whose distribution is close to the uniform [1]. This gives rise to the question of how to choose the threshold for a one-bit quantizer in order to optimize the capacity of the corresponding channel. This is a fundamental but very difficult question, which as of today seems to be unsolved in general, see [2], [3].

The general model is quite simple: input variable  $X$  with bounded support is subject to additive noise  $W$  of arbitrary distribution and then quantized to values 1 or 0, depending on if some threshold  $q \in \mathbb{R}$  is exceeded or not. In formal terms this reads as

$$Y = Q(X + W) \text{ with } Q(z) = \begin{cases} 0, & \text{if } z < q \\ 1, & \text{if } z \geq q \end{cases}.$$

The system model is depicted in Figure 1.

There is a vast literature on quantization, we only cite some work which is closely related to our research. Most papers focus on additive white Gaussian noise with average power constraints. For this case, the authors [4] show that for a  $K$ -bit quantizer with a precision of  $\log_2 K$  bits the capacity-achieving distribution is discrete with at most  $K + 1$  mass points. This result is refined in the present paper for the case  $K = 2$  and arbitrary noise distribution. In [2] it is shown under the same assumptions that the capacity-achieving distribution is discrete. In [5], one-bit quantization is considered as an asymmetric channel and optimal threshold values are determined numerically. The authors [6] investigate one-bit source quantization. It is shown that for a log-concave source distribution the optimal quantizer is symmetric about the origin.

The paper is structured as follows. We first outline that the optimum peak power constrained input distribution is discrete and concentrated on two extreme points. Thereafter, structural properties of the capacity like symmetry, monotonicity and convexity are summarized. On the basis of these results, as

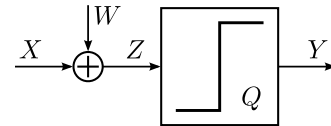


Fig. 1: The system model: some real input  $X$  is subject to additive noise  $W$  and is quantized to yield binary output  $Y$ .

the main contribution of this paper, we explicitly determine the optimum threshold value  $q^*$  in closed form for uniformly distributed noise, which against intuition is not the midpoint between the support points of the capacity-achieving input distribution. This fact also holds true for any noise distribution with sufficiently steep slope of the noise density. Finally, we present some numerical results and compare the asymmetric quantizer with the symmetric one.

## II. NOTATION AND PREREQUISITES

Self-information is denoted as

$$\rho_a(q) = -q \log_a q, \quad q \geq 0, \quad (1)$$

and the binary entropy function as

$$\begin{aligned} h_a(p) &= -p \log_a p - (1-p) \log_a (1-p) \\ &= \rho_a(p) + \rho_a(1-p), \quad 0 \leq p \leq 1, \end{aligned} \quad (2)$$

where  $a > 1$  denotes the base of the logarithm. It is well-known that both  $\rho_a(q)$  and  $h_a(p)$  are strictly concave functions of their arguments  $q$  and  $p$ , respectively. The first derivatives of the self-information and the binary entropy function are obtained as  $\rho'_a(q) = -\log_a(qe)$  and  $h'_a(p) = \log_a\left(\frac{1-p}{p}\right)$ . We will use the Kullback-Leibler divergence between  $(p, 1-p)$  and  $(q, 1-q)$ ,  $0 \leq p, q \leq 1$ , denoted by

$$D_a(p||q) = p \log_a\left(\frac{p}{q}\right) + (1-p) \log_a\left(\frac{1-p}{1-q}\right). \quad (3)$$

When applying the natural logarithm of base  $e$  we simply omit the subscript base.

We assume a discrete-time memoryless channel. Real input  $X$  with cumulative distribution function (CDF)  $F(x)$  is subject to additive noise  $W$  with density function  $\varphi(w)$  (if exists) and corresponding CDF  $\Phi(w)$ .  $X$  and  $W$  are assumed to be stochastically independent. The noisy signal  $Z = X + W$  is quantized by a binary quantizer  $Q$  with threshold  $q$  as

$Q(z) = 1$ , if  $z > q$  and  $Q(z) = 0$ , otherwise. The quantized output reads, cf. Fig. 1,

$$Y = Q(X + W). \quad (4)$$

Mutual information between input  $X$  and output  $Y$  is obtained as, cf. [7],

$$\begin{aligned} I_{X;Y} &= H(Y) - H(Y|X) \\ &= h_a\left(\int \Phi(q-x)dF(x)\right) - \int h_a(\Phi(q-x))dF(x). \end{aligned} \quad (5)$$

Mutual information is hence a function of the input distribution  $F$ , the noise distribution  $\Phi$ , and the quantization threshold  $q$ . This motivates the notation  $I_{X;Y} = I(F, \Phi, q)$ .

It is well-known that  $I(F, \Phi, q)$  is a concave function of  $F$  and a convex function of  $\Phi$ , cf. [8]. Our main goal in the present paper is to investigate the difficult optimization problem

$$\sup_q \sup_F I(F, \Phi, q) \quad (6)$$

for certain noise distributions  $\Phi$ .

In case that the input distribution is discrete with  $m$  support points  $x_1, \dots, x_m$  and probabilities  $\mathbf{p} = (p_1, \dots, p_m)$ , mutual information (5) may be written as

$$I(\mathbf{p}, \gamma) = h_a\left(\sum_{i=1}^m p_i \gamma_i\right) - \sum_{i=1}^m p_i h_a(\gamma_i). \quad (7)$$

where we have used  $\gamma = (\gamma_1, \dots, \gamma_m)$  with  $\gamma_i = \Phi(q - x_i)$ ,  $1 \leq i \leq m$ .

### III. A CLOSED-FORM FORMULA FOR THE CAPACITY-ACHIEVING INPUT DISTRIBUTION

In [9] we have given an elegant proof that the capacity-achieving distribution is discrete whenever the noise distribution is continuous.

**Theorem 1.** Assume that the noise CDF  $\Phi$  is continuous. Then for any continuous input distribution  $F$  with bounded support there exists a discrete distribution  $F_d$  with finitely many support points such that  $I(F, \Phi, q) \leq I(F_d, \Phi, q)$ .

From Theorem 1 it becomes clear that for any given threshold  $q$  the optimum input distribution is discrete with support points  $x_1 < \dots < x_m$  and probabilities  $p_1, \dots, p_m$ . Moreover, the capacity-achieving distribution is concentrated on the extreme points  $x_1$  and  $x_m$ . The corresponding probabilities and the capacity can be determined explicitly, as is summarized in the following theorem. For a proof of a modified version see, e.g., [3], [7].

**Theorem 2.** For any fixed support points  $x_1 < \dots < x_m$  and any threshold  $q$  the capacity-achieving distribution  $\mathbf{p}^*$  is concentrated on the extreme support points  $x_1$  and  $x_m$  with probabilities

$$p_1^* = \frac{1 - (1 + a^s)\gamma_m}{(1 + a^s)(\gamma_1 - \gamma_m)} \quad \text{and} \quad p_m^* = \frac{(1 + a^s)\gamma_1 - 1}{(1 + a^s)(\gamma_1 - \gamma_m)}. \quad (8)$$

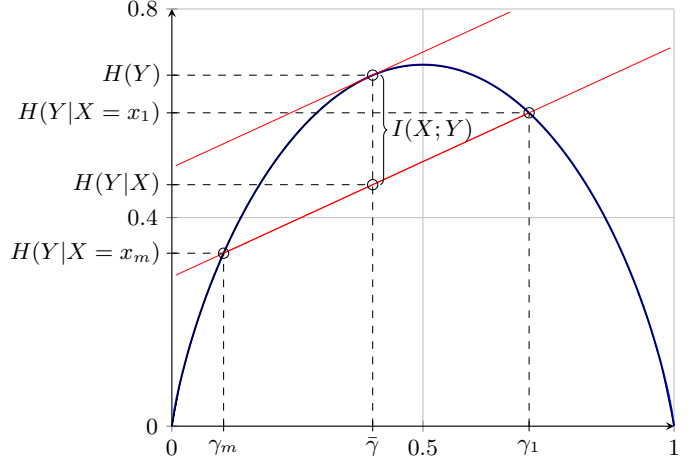


Fig. 2: The binary entropy function  $h$ , the tangent line at  $\bar{\gamma}$  and relations to entropy and mutual information.

The corresponding channel capacity is given by

$$\max_{\mathbf{p}} I(\mathbf{p}, \gamma) = \log_a(1 + a^s) - (s + t) \quad (9)$$

with constants

$$s = \frac{h_a(\gamma_1) - h_a(\gamma_m)}{\gamma_1 - \gamma_m} \quad \text{and} \quad t = \frac{\gamma_1 h_a(\gamma_m) - \gamma_m h_a(\gamma_1)}{\gamma_1 - \gamma_m}. \quad (10)$$

Tedious elementary algebra leads to the following representations of the capacity as a function of  $(\gamma_1, \gamma_m)$ .

$$\begin{aligned} C(\gamma_1, \gamma_m) &= I(\mathbf{p}^*, \mathbf{x}^*, q) \\ &= \log_a\left(e^{-\frac{(1-\gamma_m)h(\gamma_1)-(1-\gamma_1)h(\gamma_m)}{\gamma_1-\gamma_m}} + e^{-\frac{\gamma_1 h(\gamma_m)-\gamma_m h(\gamma_1)}{\gamma_1-\gamma_m}}\right) \\ &= \log_a\left(\gamma_1 e^{-\frac{1-\gamma_1}{\gamma_1-\gamma_m} D(\gamma_m \| \gamma_1)} + (1-\gamma_m) e^{-\frac{\gamma_m}{\gamma_1-\gamma_m} D(\gamma_1 \| \gamma_m)}\right) \\ &= \log_a\left(e^{\frac{(1-\gamma_1)(1-\gamma_m)}{\gamma_1-\gamma_m} \int_{\gamma_m}^{\gamma_1} \frac{\log(\gamma) d\gamma}{(1-\gamma)^2}} + e^{\frac{\gamma_m \gamma_1}{\gamma_1-\gamma_m} \int_{\gamma_m}^{\gamma_1} \frac{\log(1-\gamma) d\gamma}{\gamma^2}}\right), \end{aligned} \quad (11)$$

which reveals inherent symmetry properties. Equivalently, we have a more compact representation as

$$C(\gamma_1, \gamma_m) = h_a(\bar{\gamma}) - \left(\frac{\bar{\gamma} - \gamma_m}{\gamma_1 - \gamma_m} h_a(\gamma_1) + \frac{\gamma_1 - \bar{\gamma}}{\gamma_1 - \gamma_m} h_a(\gamma_m)\right) \quad (12)$$

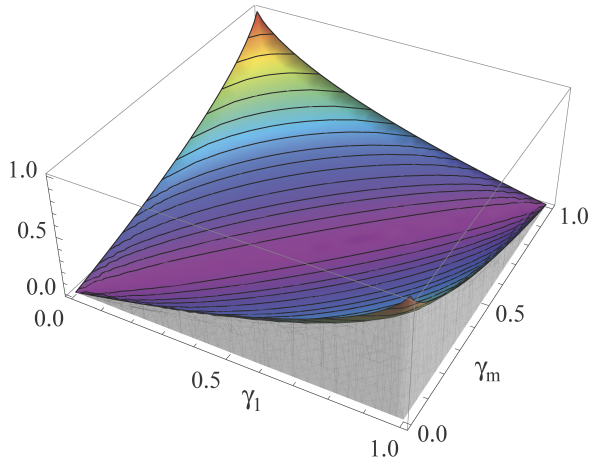
in which the term

$$\bar{\gamma} = \bar{\gamma}(\gamma_1, \gamma_m) = \left(1 + e^{\frac{h(\gamma_1) - h(\gamma_m)}{\gamma_1 - \gamma_m}}\right)^{-1} \quad (13)$$

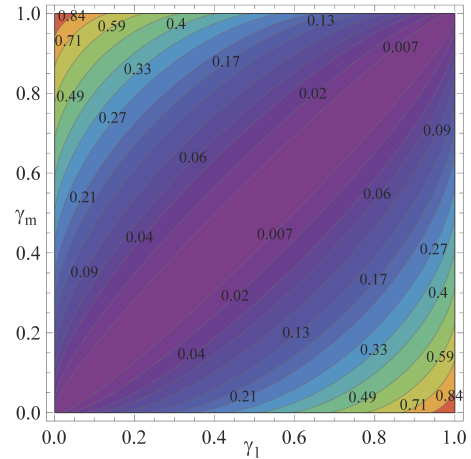
is used. Note that  $\bar{\gamma}$  is identical to the solution of  $h'(\bar{\gamma}) = \frac{h(\gamma_1) - h(\gamma_m)}{\gamma_1 - \gamma_m}$ . By this, the optimum probabilities in (8) may be written as

$$p_1^* = \frac{\bar{\gamma} - \gamma_m}{\gamma_1 - \gamma_m} \quad \text{and} \quad p_m^* = \frac{\gamma_1 - \bar{\gamma}}{\gamma_1 - \gamma_m}. \quad (14)$$

Capacity  $C(\gamma_1, \gamma_m)$  is depicted as a function of  $(\gamma_1, \gamma_m)$  in Figure 3. By formulae (12) and (13) the problem of



(a) 3d-visualization with contour lines



(b) Representation by contour lines (top-view)

Fig. 3: Channel capacity  $C(\gamma_1, \gamma_m)$  from (11) as a function of  $(\gamma_1, \gamma_m)$ .

determining the capacity-achieving input for a fixed threshold  $q$  has an intuitive graphical representation as is shown in Figure 2.

From the above representation it becomes clear that optimizing capacity with respect to threshold  $q$  is an extremely demanding problem whose solution to the best knowledge of the authors is unknown. In the next section we determine the optimum threshold for a certain class of noise distributions, a typical representative of which is the uniform distribution.

However,  $C(\gamma_1, \gamma_m)$  possesses a number of useful structural properties which are summarized in the following theorem and used later for showing optimality of thresholds for uniform noise distributions. A detailed proof will be presented in an accompanying publication.

**Theorem 3.** Channel capacity  $C(\gamma_1, \gamma_m)$  as a function of  $(\gamma_1, \gamma_2)$  has the following properties.

- $C(\gamma_1, \gamma_m)$  is symmetric in the sense that  $C(\gamma_1, \gamma_m) = C(\gamma_m, \gamma_1) = C(1 - \gamma_m, 1 - \gamma_1) = C(1 - \gamma_1, 1 - \gamma_m)$ .
- $C(\gamma_1, \gamma_m)$  is a strictly increasing function of  $\gamma_1$  and a strictly decreasing function of  $\gamma_m$ ,  $0 \leq \gamma_m < \gamma_1 \leq 1$ .
- $C(\gamma_1, \gamma_m)$  is a convex function of  $(\gamma_1, \gamma_m) \in [0, 1]^2$ . It is even strictly convex whenever  $\gamma_1 \neq \gamma_m$ .

As we have seen so far, for any support points  $-\infty < x_1 < \dots < x_m < \infty$  and any fixed threshold  $q$  the capacity-achieving input distribution is only concentrated on both extreme support points  $x_1$  and  $x_m$ . This allows us to interpret the one-bit quantizer as a binary asymmetric channel (BAC). The corresponding transition matrix is given by

$$\begin{pmatrix} 1 - \Phi(q - x_m) & \Phi(q - x_m) \\ 1 - \Phi(q - x_1) & \Phi(q - x_1) \end{pmatrix}, \quad (15)$$

where the entry in the  $x^{\text{th}}$  row and the  $y^{\text{th}}$  column denotes the conditional probability that  $y$  is received when  $x$  is sent. This relationship is shown in Fig. 4. Related early works on determining the capacity of a BAC are [10]–[15].

#### IV. OPTIMUM THRESHOLDS ARE ASYMMETRIC FOR UNIFORM NOISE

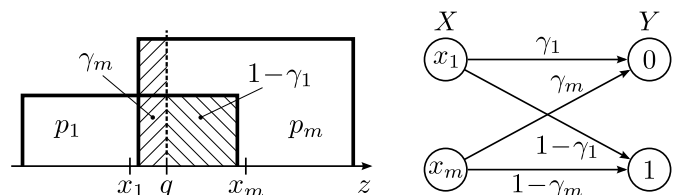
In order to find the optimum threshold  $q$ , the following optimization problem must be solved.

$$\begin{aligned} \max_{q \in \mathbb{R}} C(\gamma_1, \gamma_m) \\ \text{s. t. } \gamma_1 = \Phi(q - x_1) \text{ and } \gamma_m = \Phi(q - x_m). \end{aligned} \quad (16)$$

We will deal with the case of uniformly distributed noise with CDF

$$\Phi(w) = \begin{cases} 0, & w \leq u_\ell, \\ \frac{w - u_\ell}{u_r - u_\ell}, & u_\ell < w \leq u_r, \\ 1, & u_r < w, \end{cases} \quad (17)$$

with finite support interval  $[u_\ell, u_r]$ . By means of Proposition 3 an explicit solution of (16) can be found. Two cases are considered separately, firstly  $u_r - u_\ell < x_m - x_1$ , and secondly  $u_r - u_\ell \geq x_m - x_1$ . Both cases are summarized in Table I and II. It is easy to show that for degenerate subcases, where both  $\Phi(q - x_1)$  and  $\Phi(q - x_m)$  are equal to zero or one, mutual information is equal to zero, cf. (7).



(a) Density of  $Z = X + W$  for a uniformly distributed noise  $W$  with threshold  $q$  and probabilities  $p_1$ ,  $p_m$ ,  $\gamma_m$ , and  $1 - \gamma_m$  describing the different areas.

(b) Binary asymmetric channel with input  $X$ , output  $Y$ , and transition probabilities.

Fig. 4: Input distribution of the quantizer and the corresponding model by a BAC.

TABLE I: Overview of possible cases for a uniform noise distribution with  $u_r - u_\ell < x_m - x_1$ .

range of $q$	$\Phi(q - x_1)$	$\Phi(q - x_m)$
$q \leq u_\ell + x_1$	0	0
$u_\ell + x_1 < q \leq u_r + x_1$	$\frac{q - x_1 - u_\ell}{u_r - u_\ell}$	0
$u_r + x_1 < q \leq u_\ell + x_m$	1	0
$u_\ell + x_m < q \leq u_r + x_m$	1	$\frac{q - x_m - u_\ell}{u_r - u_\ell}$
$u_r + x_m < q$	1	1

We first deal with the case  $u_r - u_\ell < x_m - x_1$ . The subcase  $\Phi(q - x_1) = 1$  and  $\Phi(q - x_m) = 0$  obviously yields  $C(q) = \log_a 2$  for  $u_r + x_1 < q \leq u_\ell + x_m$ . For  $u_\ell + x_1 < q \leq u_r + x_1$ , it holds that  $C(\gamma_1, \gamma_m) = C(\frac{q - x_1 - u_\ell}{u_r - u_\ell}, 0)$ . Since  $\gamma_m = 0$  is fixed, we can use Theorem 3 b) to maximize the channel capacity by maximizing  $\gamma_1$ . To maximize  $\gamma_1$  we only need to maximize  $q$  within its boundaries. Hence, the maximum is achieved for  $q^* = u_r + x_1$  with value  $C(1, 0) = \log_a 2$ .

Analogously, for the subcase  $u_\ell + x_m < q \leq u_r + x_m$ , the monotonicity property in Theorem 3 b) ensures that channel capacity is maximum for a minimal  $\gamma_m$ . Hence,  $C(1, \frac{q - x_m - u_\ell}{u_r - u_\ell}) \leq C(1, 0) = \log_a 2$  is attained at  $q^* = u_\ell + x_m$ .

In summary, if  $u_r - u_\ell < x_m - x_1$  then the optimum capacity  $C^* = \log_a 2$  is attained at any  $q^* \in [u_r + x_1, u_\ell + x_m]$ .

Note that the optimal solution is not unique, since the shifted noise densities do not have overlapping support. From  $\Phi(q^* - x_1) = 1$  and  $\Phi(q^* - x_m) = 0$  with the aid of (13) and (14), the optimal probabilities are derived as  $p_1^* = \frac{1}{2}$  and  $p_m^* = \frac{1}{2}$ .

TABLE II: Overview of possible cases for a uniform noise distribution with  $u_r - u_\ell \geq x_m - x_1$ .

range of $q$	$\Phi(q - x_1)$	$\Phi(q - x_m)$
$q \leq u_\ell + x_1$	0	0
$u_\ell + x_1 < q \leq u_\ell + x_m$	$\frac{q - x_1 - u_\ell}{u_r - u_\ell}$	0
$u_\ell + x_m < q \leq u_r + x_1$	$\frac{q - x_1 - u_\ell}{u_r - u_\ell}$	$\frac{q - x_m - u_\ell}{u_r - u_\ell}$
$u_r + x_1 < q \leq u_r + x_m$	1	$\frac{q - x_m - u_\ell}{u_r - u_\ell}$
$u_r + x_m < q$	1	1

We now consider the remaining case  $u_r - u_\ell \geq x_m - x_1$ . By analogous methods as above the maximum of  $C(\frac{q - x_1 - u_\ell}{u_r - u_\ell}, 0)$  over  $u_\ell + x_1 < q \leq u_\ell + x_m$  is attained at  $q^* = u_\ell + x_m$  with value  $C(\frac{x_m - x_1}{u_r - u_\ell}, 0)$ . On the other hand, if  $u_r + x_1 < q \leq u_r + x_m$  then  $C(1, \frac{q - x_m - u_\ell}{u_r - u_\ell})$  is maximized at  $q^* = u_r + x_1$  with value  $C(1, \frac{u_r - u_\ell - (x_m - x_1)}{u_r - u_\ell}) = C(\frac{x_m - x_1}{u_r - u_\ell}, 0)$ , due to symmetry in Theorem 3 a).

The subcase  $u_\ell + x_m < q \leq u_r + x_1$  needs a different approach. Since the difference  $\Phi(q - x_1) - \Phi(q - x_m) = \frac{q - x_1 - u_\ell}{u_r - u_\ell} - \frac{q - x_m - u_\ell}{u_r - u_\ell} = \frac{x_m - x_1}{u_r - u_\ell}$  is independent of  $q$ , monotonicity arguments do not apply for the channel capacity over  $q \in [u_\ell + x_m, u_r + x_1]$ . Convexity of  $C(\gamma_1, \gamma_m)$  as stated in Theorem 3 c), however, yields that the maximum is attained at a boundary point of  $q$ . Because of symmetry, cf. Theorem 3 a),

both values of the capacity  $C(\frac{q - x_1 - u_\ell}{u_r - u_\ell}, \frac{q - x_m - u_\ell}{u_r - u_\ell})$  are equal at the boundary points  $q = u_\ell + x_m$  and  $q = u_r + x_1$  such that the optimum is attained at each  $q^* \in \{u_\ell + x_m, u_r + x_1\}$ . The corresponding capacity coincides with the capacity of the Z-channel and reads as

$$C^* = \log_a \left( 1 + e^{-\frac{h(\gamma_1^*)}{\gamma_1^*}} \right) \quad (18)$$

with  $\gamma_1^* = \frac{x_m - x_1}{u_r - u_\ell}$ . Note that in the case  $u_r - u_\ell \geq x_m - x_1$  the BAC degenerates to a Z-channel in which one of the input symbols is always communicated error-free while the other symbol is communicated with loss (note also the importance of the erasures-only capacity [16], [17] which is equal to the Shannon's capacity for the Z-channel). The corresponding probabilities are obtained as

$$p_1^* = \frac{\bar{\gamma}^*}{\gamma_1^*} \quad \text{and} \quad p_m^* = 1 - \frac{\bar{\gamma}^*}{\gamma_1^*} \quad (19)$$

with

$$\bar{\gamma}^* = \frac{e^{-\frac{h(\gamma_1^*)}{\gamma_1^*}}}{C^*}. \quad (20)$$

Note that the above approach can be used for other noise distributions with bounded support to show that the optimal threshold is asymmetric. Table III lists some examples of noise distributions with bounded support, which have an asymmetric optimal threshold  $q^*$ .

TABLE III: Examples of noise distributions with bounded support.

$\Phi(w)$	support	behavior of $\Phi$	$q^*$
$\sin(w)$	$w \in [0, \frac{\pi}{2}]$	concave	$x_m$
$1 - \cos(w)$	$w \in [0, \frac{\pi}{2}]$	convex	$x_1 + \frac{\pi}{2}$
$\frac{\sqrt{w}}{2}, w \in [0, 1]$ $1 - \frac{\sqrt{2-w}}{2}, w \in [1, 2]$	$w \in [0, 2]$	-	$x_m$

## V. NUMERICAL RESULTS

In this section, we present selected numerical results to provide insight into the channel capacity of the one-bit quantizer. For the following results we consider the case  $x_1 = -x_m = -1$  for the signal constellation of the input  $X$ , which corresponds to a constant input power one for any choice of the symbol probabilities, i.e.,  $E(X^2) = p_1 x_1^2 + p_m x_m^2 = 1$ . We also assume zero-mean uniformly distributed noise  $W$ . The power  $E(W^2)$  will be changed by varying the support to obtain different signal-to-noise ratios  $\text{SNR} = \frac{E(X^2)}{E(W^2)}$ . For some computations the noise power is set to discrete values in  $\{10, 1, \frac{1}{2}, \frac{1}{3}, \frac{1}{10}\}$ , corresponding to a signal-to-noise ratio  $\text{SNR} \in \{\frac{1}{10}, 1, 2, 3, 10\}$ . These cases are indicated by colors red, magenta, green, cyan and blue, respectively. We will also sometimes consider the signal-to-noise ratio over a whole interval, e.g.,  $\text{SNR} \leq 10$ . The base of the logarithm is chosen as  $a = 2$ .

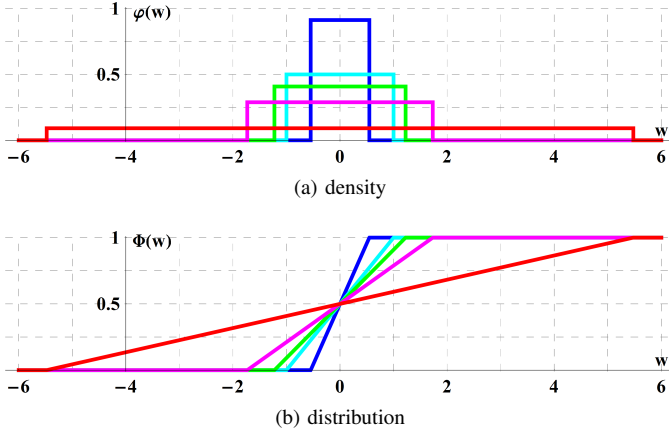


Fig. 5: Density and distribution of uniformly distributed noise for different noise powers  $\{\frac{1}{10}, \frac{1}{3}, \frac{1}{2}, 1, 10\}$ .

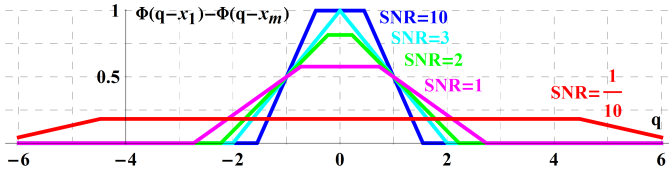


Fig. 6: The difference  $\Phi(q - x_1) - \Phi(q - x_m)$  of the Noise CDFs as a function of the threshold  $q$  for different signal-to-noise ratios  $\text{SNR} \in \{\frac{1}{10}, 1, 2, 3, 10\}$ .

In Fig. 5 the density  $\varphi(w)$  and the distribution function  $\Phi(w)$  for the five noise powers are shown. In Fig. 6 the difference  $\Phi(q - x_1) - \Phi(q - x_m)$  is plotted to identify the cases  $u_r - u_\ell < x_m - x_1$ ,  $u_r - u_\ell > x_m - x_1$  and  $u_r - u_\ell = x_m - x_1$ . For  $\text{SNR} = 10$  the case  $u_r - u_\ell < x_m - x_1$  is shown in blue. In contrast, the case  $u_r - u_\ell > x_m - x_1$  is represented by  $\text{SNR} \in \{\frac{1}{10}, 1, 2\}$  in red, magenta and green colors, respectively. The case  $u_r - u_\ell = x_m - x_1$  is attained for  $\text{SNR} = 3$  and depicted in cyan.

The contours of the capacity  $C(\gamma_1, \gamma_m)$  in the region  $(\gamma_1, \gamma_m) \in [0, 1]^2$ , cf. (11), along with the trajectories  $(\gamma_1, \gamma_m) = (\Phi(q - x_1), \Phi(q - x_m))$ ,  $q \in (-\infty, \infty)$ , are plotted in Fig. 7. Note that on the diagonal line between  $(0, 0)$  and  $(1, 1)$  the capacity is zero while on the corners  $(0, 1)$  and  $(1, 0)$  the capacity is equal to  $\log_a 2$ . All trajectories start at  $(0, 0)$  for  $q \mapsto -\infty$  and end in  $(1, 1)$  for  $q \mapsto \infty$ . Each trajectory remains parallel to the coordinate axes until the maximum capacity is attained, which is marked by a circle in corresponding color. Then each trajectory runs diagonal to a circle on the perpendicular side of the region, where again the maximum capacity is attained. Departing from the circles in either direction on the trajectory decreases the capacity. From the second circle each trajectory again remains parallel to the coordinate axes. In the case  $u_r - u_\ell \leq x_m - x_1$  both circles are degenerated to a single circle, that is located on the corner of the region (the cyan circle lies within the blue circle). The behavior of the capacity as a function of the threshold  $q$  can also be read from Fig. 8. For  $q = q_c = \mu + \frac{x_1 + x_m}{2}$  the quantizer

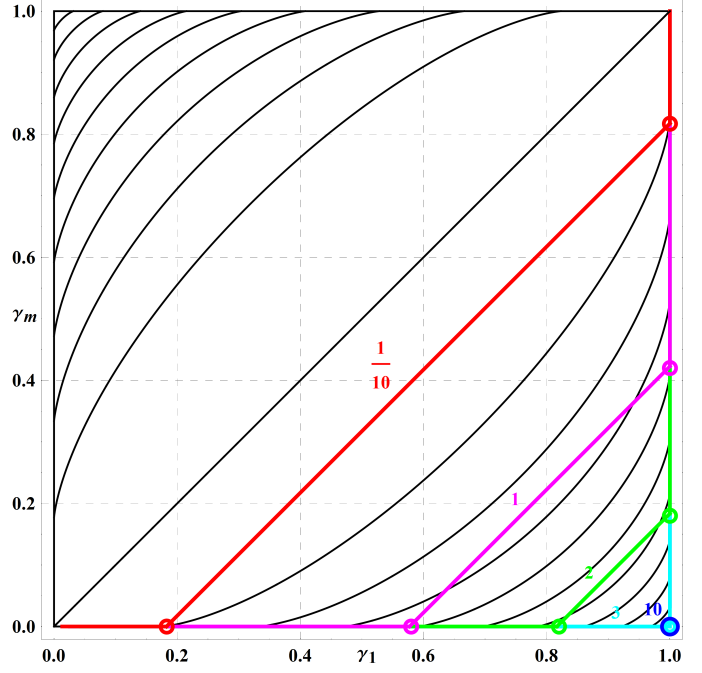


Fig. 7: Capacity contours together with trajectories of uniformly distributed noise for different signal-to-noise ratios  $\text{SNR} \in \{\frac{1}{10}, 1, 2, 3, 10\}$ .

becomes symmetric which corresponds with a BSC, where  $q_c$  is the centroid of the capacity curves. For this choice of the threshold (here  $q_c = 0$ ) the capacity attains a local minimum. The difference of the capacities  $C(q^*) - C(q = q_c)$  seems to be large in the region where the signal-to-noise ratio is intermediate. This region is the most relevant for optimizing the threshold  $q$  in practice.

It is interesting to see that the maximum capacity of  $\log_a 2$  is attained for  $\text{SNR} = 3 \approx 4.77\text{dB}$  and for any further increase of the signal-to-noise ratio the capacity will remain constant.

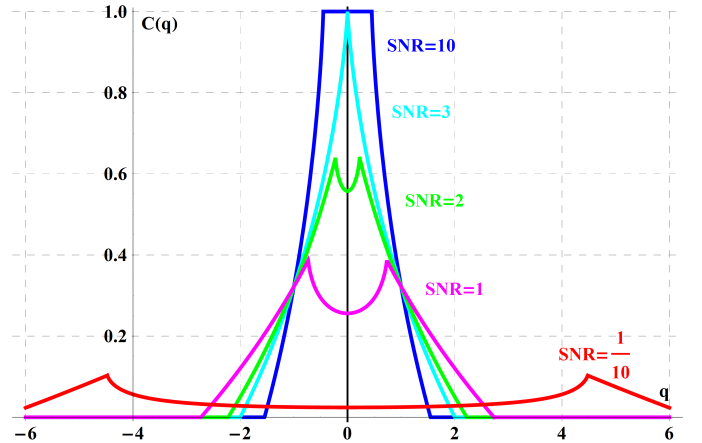
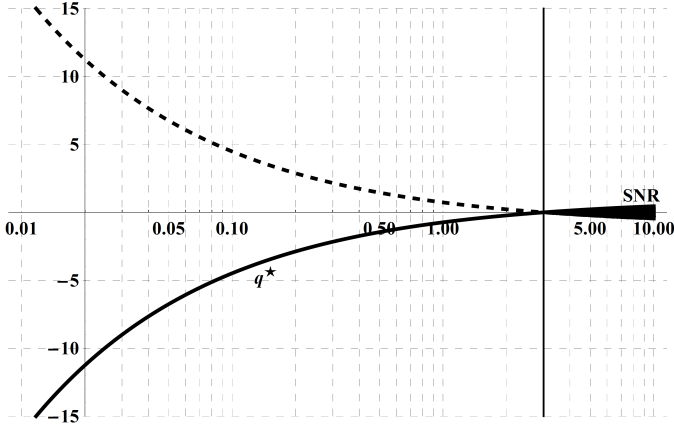
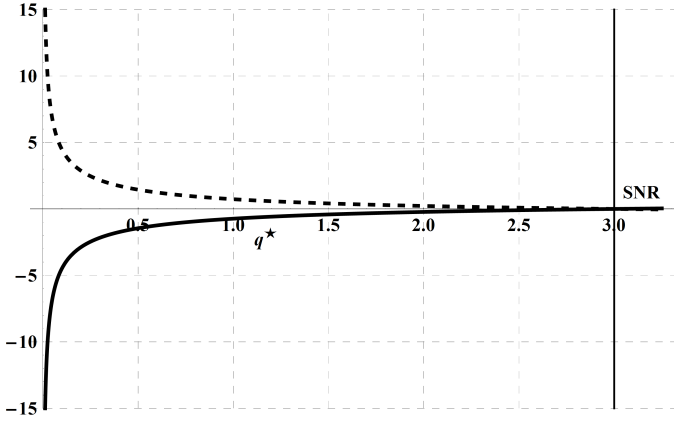


Fig. 8: The capacity  $C(q)$  for uniformly distributed noise as a function of the threshold  $q$  for different signal-to-noise ratios  $\text{SNR} \in \{\frac{1}{10}, 1, 2, 3, 10\}$ .



(a) logarithmic



(b) linear

Fig. 9: Optimal threshold  $q^*$  over the signal-to-noise ratio on a logarithmic and linear scale.

We will highlight this signal-to-noise limitation by a thin black vertical line in the following.

To obtain deeper insight we calculate the optimal threshold  $q^*$  along with  $\gamma_1^* = \Phi(q^* - x_1)$  and  $\gamma_m^* = \Phi(q^* - x_m)$  as  $q^* = 1 - \sqrt{3/\text{SNR}}$ ,  $\gamma_1^* = \sqrt{\text{SNR}/3}$  and  $\gamma_m^* = 0$ . Note that another optimal value for all  $q$ ,  $\gamma_1$  and  $\gamma_m$  exist, which we neglect to consider because of the symmetry. From these optimal values we in addition can determine  $C(q^*)$ ,  $p_1^*$ ,  $p_m^*$  and  $\bar{\gamma}^*$  as given by (18)–(20), which are still complicated equations. It is easy to show that for  $\text{SNR} \mapsto 0$  we obtain the approximations

$$\bar{\gamma}^* \simeq \frac{1}{e} \sqrt{\frac{\text{SNR}}{3}}, \quad (21a)$$

$$p_1^* \simeq \frac{1}{e} + \frac{e-2}{2e^2} \sqrt{\frac{\text{SNR}}{3}}, \quad (21b)$$

$$p_m^* \simeq 1 - \frac{1}{e} - \frac{e-2}{2e^2} \sqrt{\frac{\text{SNR}}{3}}, \quad (21c)$$

$$C(q^*) \simeq \frac{\log_a e}{e} \sqrt{\frac{\text{SNR}}{3}}. \quad (21d)$$

For  $\text{SNR} \mapsto 3$  we similarly obtain the approximations

$$\bar{\gamma}^* \simeq \frac{1}{2} - \frac{1 - \sqrt{\frac{\text{SNR}}{3}}}{4} \left( 1 - \log \left( 1 - \sqrt{\frac{\text{SNR}}{3}} \right) \right), \quad (22a)$$

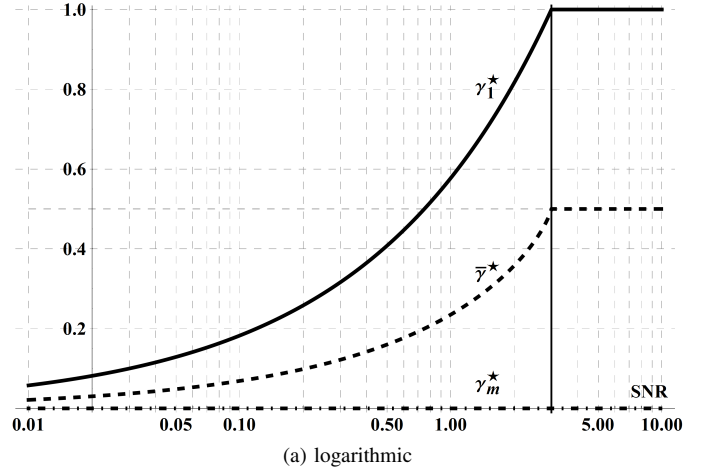
$$p_1^* \simeq \frac{1}{2} \sqrt{\frac{3}{\text{SNR}}} - \frac{\sqrt{\frac{3}{\text{SNR}} - 1}}{4} \left( 1 - \log \left( 1 - \sqrt{\frac{\text{SNR}}{3}} \right) \right), \quad (22b)$$

$$p_m^* \simeq 1 - \frac{1}{2} \sqrt{\frac{3}{\text{SNR}}} + \frac{\sqrt{\frac{3}{\text{SNR}} - 1}}{4} \left( 1 - \log \left( 1 - \sqrt{\frac{\text{SNR}}{3}} \right) \right), \quad (22c)$$

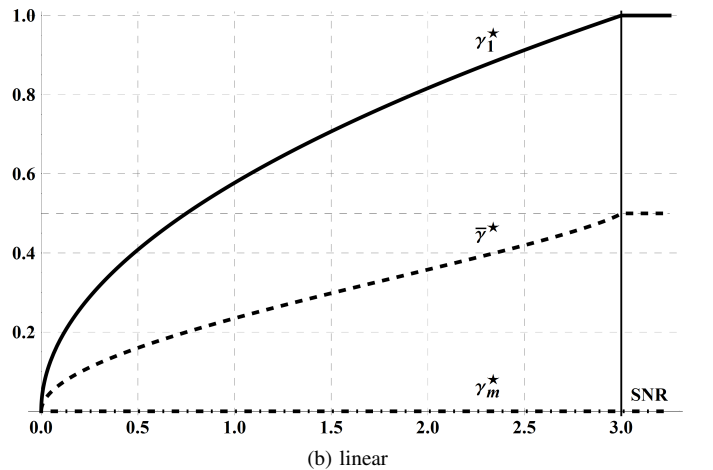
$$C(q^*) \simeq \log_a 2 + \frac{1 - \sqrt{\frac{\text{SNR}}{3}}}{2} \log_a \left( \frac{1 - \sqrt{\frac{\text{SNR}}{3}}}{e} \right). \quad (22d)$$

In Fig. 9 the optimal thresholds  $q^*$  over the signal-to-noise ratio SNR are shown. The optimal threshold is a hyperbolic function over the whole range of the signal-to-noise ratio except of  $\text{SNR} > 3$ . For  $\text{SNR} > 3$  the optimal threshold can be chosen arbitrarily between  $1 - \sqrt{3/\text{SNR}}$  and  $\sqrt{3/\text{SNR}} - 1$ . The behavior for  $\text{SNR} > 3$  can be better recognized on a logarithmic scale.

Fig. 10 shows the optimal values  $\gamma_1^*$ ,  $\bar{\gamma}^*$  and  $\gamma_m^*$  over the signal-to-noise ratio if  $q^* = 1 - \sqrt{3/\text{SNR}}$  is selected. As stated in (21), the value  $\bar{\gamma}^*$  converges for  $\text{SNR} \mapsto 0$  to  $\gamma_1^*$  up to a constant factor. Furthermore, the slope of  $\gamma_1^*$  at  $\text{SNR} = 0$  is infinite due to the square root. This behavior has a positive effect on the capacity gain as we will see later.

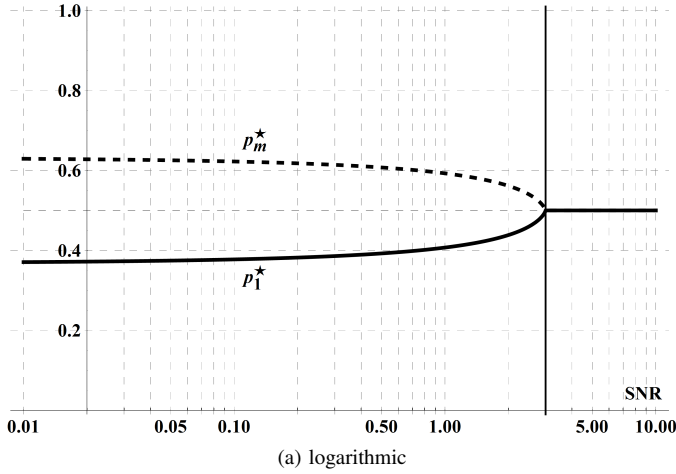


(a) logarithmic

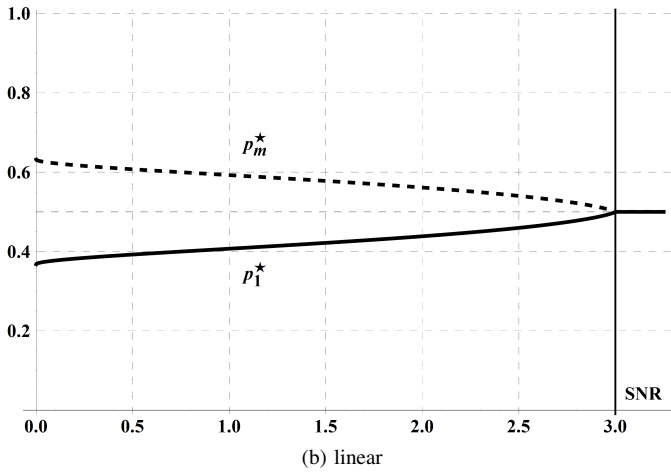


(b) linear

Fig. 10: Optimal values  $\gamma_1^*$ ,  $\bar{\gamma}^*$  and  $\gamma_m^*$  over the signal-to-noise ratio on a logarithmic and linear scale.



(a) logarithmic



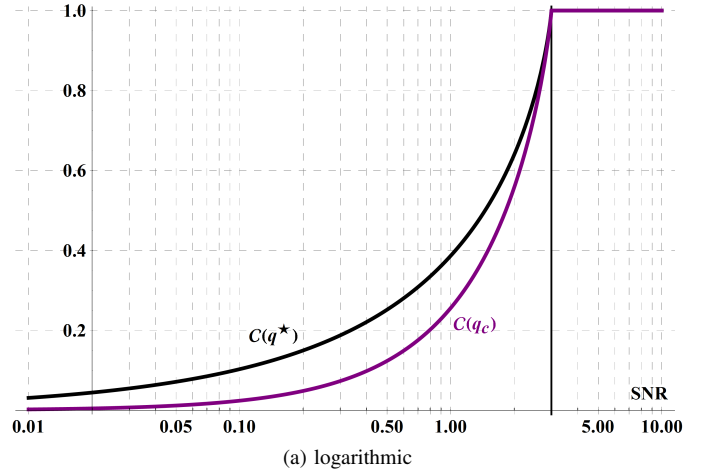
(b) linear

Fig. 11: Optimal input-probabilities  $p_1^*$  and  $p_m^*$  over the signal-to-noise ratio in logarithmic and linear scale.

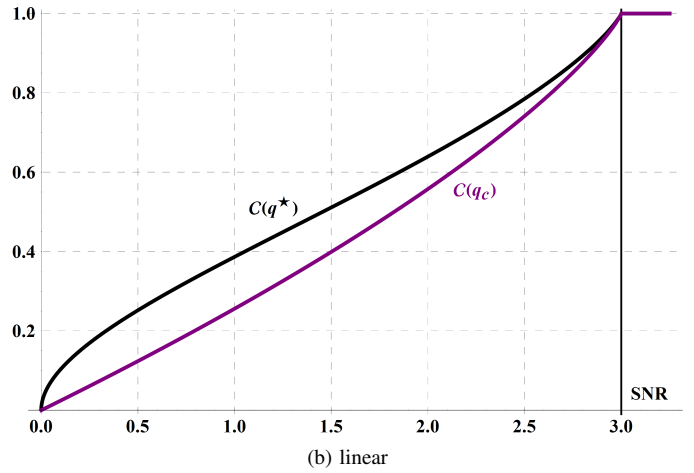
In Fig. 11 the optimal input probabilities over the signal-to-noise ratio are shown. It is interesting that the variation range of the probabilities is bounded by  $\frac{1}{e}$  and  $\frac{1}{2}$ . For  $p_1^*$  the lower bound is attained as  $\text{SNR} \mapsto 0$  while the upper bound is achieved as  $\text{SNR} \mapsto 3$ , see (21) and (22).

Finally, the optimal capacity is depicted over the signal-to-noise ratio in Fig. 12. As can be seen the maximum increase of capacity occurs as  $\text{SNR} \mapsto 0$ , since the curve is concave in this region. In addition, the capacity  $C(q_c)$  of the centroid is shown at which the capacity attains a local minimum. As mentioned before, the difference between them is large for mid-range values of the signal-to-noise ratio. This difference reinforces that optimal one-bit quantizers are asymmetric for additive uniform noise.

In Fig. 13, the density at the input  $Z = X + W$  of the quantizer for an optimal constellation of the input signal  $X$  with probabilities  $p_1^*$  and  $p_m^*$  along with the position of the optimal threshold  $q^*$  for two different signal-to-noise ratios  $\text{SNR} \in \{\frac{1}{10}, 3\}$  is depicted. For the choice  $q^* = 1 - \sqrt{3/\text{SNR}}$  the symbol  $x_1 = -1$  has a lower probability of occurrence than  $x_m = +1$ , i.e.,  $p_1^* < p_m^*$  for all  $\text{SNR} < 3$ . Due to the



(a) logarithmic



(b) linear

Fig. 12: Optimal capacity  $C(q^*)$  and the capacity  $C(q_c)$  of the centroid over the signal-to-noise ratio in logarithmic and linear scale.

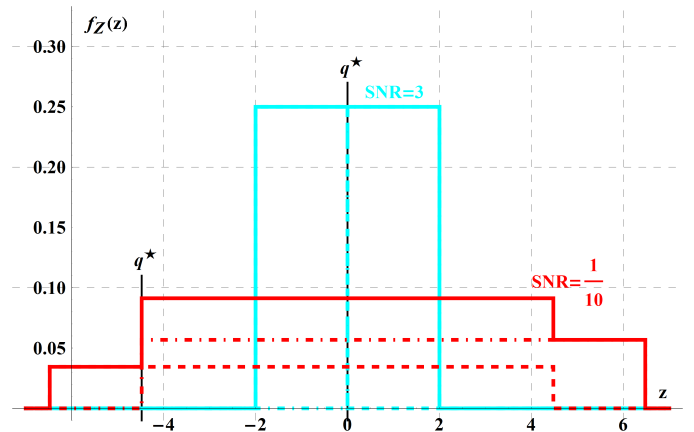


Fig. 13: Density at the input  $Z = X + W$  of the quantizer for optimal constellation of the input signal  $X$  with probabilities  $p_1^*$  and  $p_m^*$  along with the position of the optimal threshold  $q^*$  for two different signal-to-noise ratios  $\text{SNR} \in \{\frac{1}{10}, 3\}$ .

position of  $q^*$ , a transmitted symbol  $x_m$  is always received error-free while symbol  $x_1$  may be erroneously decoded as  $x_m$  at the output of the quantizer. This demonstrates the importance of the Z-channel as a reasonable transmission model whenever the noise has bounded support.

## VI. CONCLUSION

In this paper, we have considered the one-bit output quantization of an amplitude bounded input-signal subject to arbitrary additive noise. Capacity has been represented in various ways, each demonstrating that finding the optimum quantization threshold  $q^*$  is an extremely difficult problem. For the class of uniform noise distributions, it has been shown that the optimum quantizer is asymmetric and the optimal threshold can be determined in closed-form. By numerical investigations we have also compared the optimal asymmetric quantizer with the symmetric one for obtaining detailed information about the loss in capacity.

## REFERENCES

- [1] W. Kester, "Adc input noise: The good, the bad, and the ugly. is no good noise?" *Analog Dialogue*, vol. 40, no. 1, pp. 13–17, feb 2006.
- [2] T. Koch and A. Lapidoth, "At low snr, asymmetric quantizers are better," *Information Theory, IEEE Transactions on*, vol. 59, no. 9, pp. 5421–5445, Sep. 2013.
- [3] G. Alirezaei and R. Mathar, "Optimum one-bit quantization," in *The IEEE Information Theory Workshop (ITW'15)*, Jeju Island, Korea, Oct. 2015.
- [4] J. Singh, O. Dabeer, and U. Madhow, "Communication limits with low precision analog-to-digital conversion at the receiver," in *Communications, 2007. ICC '07. IEEE International Conference on*, June 2007, pp. 6269–6274.
- [5] P. Amblard, O. Michel, and S. Morfu, "Revisiting the asymmetric binary channel: joint noise enhanced detection and information transmission through threshold devices," in *Noise in Complex Systems and Stochastic Dynamics III*, 2005, pp. 50–60.
- [6] A. Magnani, A. Ghosh, and R. M. Gray, "Optimal one-bit quantization," in *Proceedings of the Data Compression Conference, DCC'05*, Snowbird, Utah, USA, 2005.
- [7] R. Mathar and M. Dörpinghaus, "Threshold optimization for capacity-achieving discrete input one-bit output quantization," in *IEEE International Symposium on Information Theory (ISIT 2013)*, Istanbul, Turkey, Jul. 2013, pp. 1999–2003.
- [8] I. Csiszar and J. Körner, *Information Theory, Coding Theorems for Discrete Memoryless Systems*, Z. Birnbaum and E. Lukacs, Eds. Akademiai Kiado and Academic Press, 1981.
- [9] G. Alirezaei and R. Mathar, "On the discreteness of capacity-achieving input distributions with finite support," Institute for Theoretical Information Technology, RWTH Aachen University, Tech. Rep., 2015.
- [10] S. Muroga, "On the capacity of a discrete channel, i," *Journal of the Physical Society of Japan*, vol. 8, no. 4, pp. 484–494, 1953.
- [11] R. Silverman, "On binary channels and their cascades," *IRE Transactions on Information Theory*, vol. 1, no. 3, pp. 19–27, December 1955.
- [12] S. Muroga, "On the capacity of a discrete channel, ii," *Journal of the Physical Society of Japan*, vol. 11, no. 10, pp. 1109–1120, 1956.
- [13] S. Arimoto, "An algorithm for computing the capacity of arbitrary discrete memoryless channels," *Information Theory, IEEE Transactions on*, vol. 18, no. 1, pp. 14–20, Jan 1972.
- [14] R. E. Blahut, "Computation of channel capacity and rate-distortion functions," *Information Theory, IEEE Transactions on*, vol. 18, no. 4, pp. 460–473, Jul 1972.
- [15] S. Takano, "On a method of calculating the capacity of a discrete memoryless channel," *Information and Control*, vol. 29, pp. 327–336, 1975.
- [16] M. S. Pinsker and A. Y. Sheverdyaev, "Transmission capacity with zero error and erasure," *Probl. Peredachi Inf.*, vol. 6, no. 1, pp. 20–24, 1970.
- [17] I. Csiszar and P. Narayan, "Channel capacity for a given decoding metric," *IEEE Transactions on Information Theory*, vol. 41, no. 1, pp. 35–43, Jan 1995.